2.4.3.3 Photon Counting

The previous systems measure the total intensity of the detected X-ray beam, which is composed of many photons. With a sufficiently fast read-out rate (a few MHz), however, it is possible to count the number of photons and measure their individual energy. Commercial mammography systems exist that offer this *photon counting* technology. They use crystalline silicon for direct X-ray conversion and several linear detector rows to acquire a 2D image in a few seconds. An advantage of a slit-scanning technology is its superior CNR due to the efficient removal of scatter noise without the need for an anti-scatter grid. Another advantage of photon counting systems is that multiple bins of distinct energy spectra are available. This offers, for example, the possibility of spectral imaging, which is particularly promising in CT (see Section 3.5).

2.5 Image Quality

2.5.1 Resolution

The image resolution of a radiographic system depends on several factors.

- The size of the focal spot. The focal spot is the area on which the electrons hit the anode and where the X-rays originate. It is usually positioned at a large angle with the electron beam and a small angle relative to the imaging plane. This way the thermal length (physical) is much larger than the optical length (projected), which spreads the heat production over a larger thermal area, and produces a nicely focused X-ray beam.

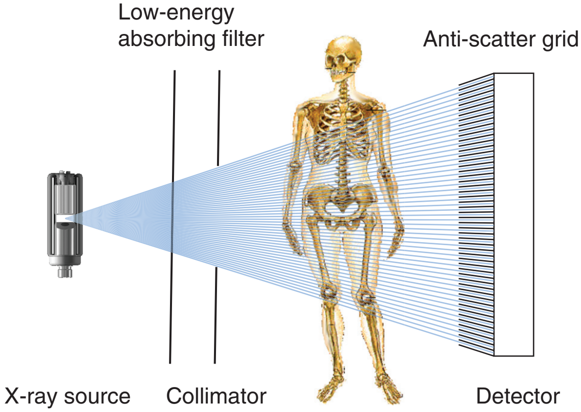

Figure 2.9 Schematic representation of the radiographic imaging chain.

- The patient. Thicker patients cause more X-ray scatter, deteriorating the image resolution. Patient scatter can be reduced by placing a collimator grid in front of the screen (see Figure 2.9). The grid allows only the photons with low incidence angle to reach the screen.
- The light scattering properties of the fluorescent screen.
- For film the resolution is mainly determined by its grain size, while for image intensifier systems and digital radiography the sampling step is the most important factor.

The resolving power, defined as the frequency where the modulation transfer function (MTF) is 10%, of clinical systems varies from 5 up to 15 lp/mm. For general-purpose digital radiography the pixel size is about 150 μm. Mammography detectors have a notably better sharpness, in the order of 75 μm. Photon counting systems with slit-scanning have a pixel size of 50 μm. Depending on the object size, images with 3000 by 3000 pixels and even more are needed.

2.5.2 Contrast

The contrast is the intensity difference in adjacent regions of the image. According to Eq. 2.7 the image intensity depends on the emitted X-ray intensity, the attenuation coefficients $\mu(E, x)$, and thicknesses of the different tissue layers encountered along the projection line. Because the attenuation coefficient depends on the energy of the X-rays, the spectrum of the beam has an important influence on the contrast. Low-energy radiation, as used in mammography, typically yields a higher contrast than high-energy radiation.

The contrast is further influenced by the detector efficiency. The higher the efficiency, the better the contrast is. In digital radiography, the image contrast can further be improved by a suitable gray value transformation (see Section 1.3.1). Note, however, that such a transformation also influences the noise, thus keeping the CNR unchanged.

2.5.3 Noise

Quantum noise, which is due to the statistical nature of X-ray photons, is typically the dominant noise factor. A photon-detecting process is essentially a Poisson process (the variance is equal to the mean). Therefore, the noise amplitude (standard deviation) is proportional to the square root of the signal amplitude, and the SNR also behaves as the square root of the signal amplitude. This explains why dose reduction does not remain unpunished in terms of image quality, as gratuitous signal reduction would reduce the SNR to an unacceptable level. Further conversions during the imaging process, such as photon–electron conversions, will add noise and further decrease the SNR.

To quantify the quality of an image detector, the *detective quantum efficiency* (DQE) is often used. The image detector is one element in the imaging chain and to specify its contribution to the SNR of an imaging process, the DQE is used, which expresses the signal-to-noise transfer through the detector. The DQE can be calculated by taking the ratio of the squared SNR at the detector output to the squared SNR of the input signal as a function of spatial frequency

$$\mathrm{DQE}(f) = \frac{\mathrm{SNR}^2_{\mathrm{out}}(f)}{\mathrm{SNR}^2_{\mathrm{in}}(f)}. \tag{2.11}$$

It is a measure of how the available signal-to-noise ratio is degraded by the detector. Several factors influence the DQE of a detector, particularly its primary interaction efficiency, its point spread function, the noise it introduces, and also the energy spectrum of the incoming X-rays. The DQE is a suitable measure to compare the overall performance of different detector technologies. Examples of the DQE as a function of frequency of different digital detector technologies for general-purpose and for mammography are illustrated in Figures 2.7 and 2.8, respectively. Figure 2.7 shows that the DQE is poorest for the powder storage phosphor, as the thin scintillator layer required to maintain good sharpness results in reduced X-ray absorption. The needle-shaped storage phosphor (CsBr-based) greatly improves X-ray absorption, giving a DQE that approaches the DQE of active matrix detectors with CsI needle phosphors. Currently, needle scintillators are the dominant X-ray conversion materials due to their excellent absorption at higher energies without excessive loss of sharpness and reasonable conversion gain fluctuation noise. Figure 2.8 shows an improved DQE at higher spatial frequencies for an a-Se mammography detector compared to scintillator-based detectors. There are two main reasons. First, the lower energies required to enhance tissue differentiation for the mammographic task result in high X-ray absorption within the a-Se layer. Operating at these lower energies means that a-Se can match the absorption efficiency of phosphor scintillators. Second, the a-Se layer has high intrinsic sharpness leading to excellent performance at higher spatial frequencies.

2.5.4 Artifacts

Although other modalities suffer more from severe artifacts than radiography, X-ray images are generally not artifact-free. Scratches in the detector, dead pixels, unread scan lines, inhomogeneous X-ray beam intensity (heel effect), afterglow, etc., are not uncommon and deteriorate the image quality.

2.6 Equipment

Let us now take a look at the complete radiographic imaging chain, which is illustrated schematically in Figure 2.9. It consists of the following elements:

- The X-ray source.
- An aluminum filter, often complemented by a copper filter. This filter removes low-energy photons, thus increasing the mean energy of the photon beam. Low-energy photons deliver doses to the patient but are useless for the imaging process because they do not have enough energy to travel through the patient and never reach the detector. Because low-energy photons are called *soft radiation* and high-energy photons *hard radiation*, this removal of low-energy photons from the beam is called *beam hardening*.
- A collimator to limit the patient area to be irradiated.
- The patient, who attenuates the X-ray beam and produces scatter. Beam hardening proceeds when the X-rays travel through the patient.
- An anti-scatter grid. This is a collimator that absorbs scatter photons. It stops photons with large incidence angle, whereas photons with small incidence angle can pass right through the grid. The grid can be made of lead, for example.
- The detector. This can be a screen–film combination in which a film is sandwiched between two screens (see Section 2.4.1.1), an image intensifier coupled to a camera (see Section 2.4.2), a storage-phosphor plate (see Section 2.4.3.1), or an active matrix flat panel detector (see Section 2.4.3.2).

Figure 2.10 shows a general-purpose radiographic room for radiography and fluoroscopy. The detector with wireless data transfer is a large-area active matrix array coupled to a needle-shaped scintillator

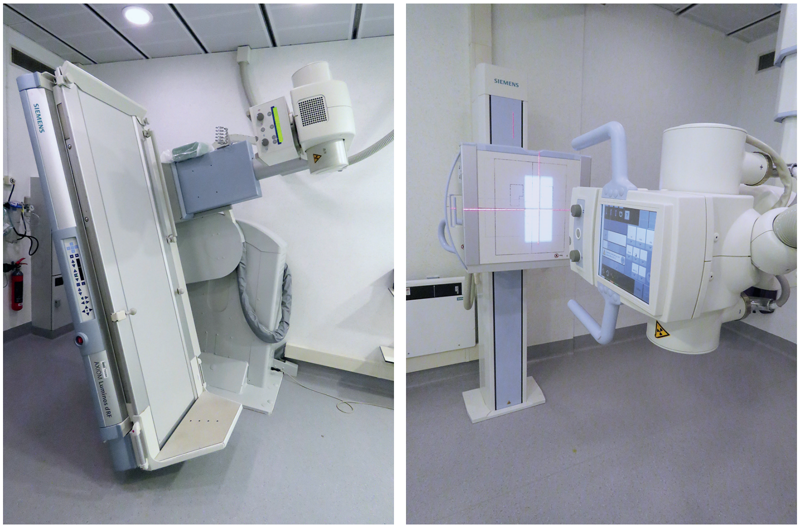
(a) (b)

Figure 2.10 Multipurpose radiographic room (Axiom Luminos dRF with second plane, Siemens Healthcare). **(a)** The table can be tilted in any orientation. The large-coverage flat detector, with needle-shaped thallium-doped cesium iodide (CsI:Tl) scintillator, can be used for both radiography and fluoroscopy. **(b)** Wall stand for full spine and long leg imaging using the same exchangeable and portable flat detector with wireless connection.

Figure 2.11 Similar system as Figure 2.10(a) but the X-ray tube is placed under the table and an easily movable detector with radiation protective shield above the table, suitable for patient-side examinations (Luminos Agile, Siemens Healthcare).

plate. The table can be tilted in any orientation (Figure 2.10(a)) and the wall stand (Figure 2.10(b)) makes full spine and long leg imaging feasible. The system in Figure 2.11 is comparable to that shown in Figure 2.10(a), but its flexible detector handling and radiation protective shield make it particularly suited for patient-side examinations. Similar detector technology is used in the mobile X-ray system shown in Figure 2.12, which can be used for fast bedside examinations.

The digital mammography system shown in Figure 2.13 employs direct X-ray conversion with amorphous selenium for an optimal detectability.

Figure 2.12 Mobile radiographic system for bedside imaging (DX-D 100, Agfa Healthcare). It uses a wireless portable detector with needle-shaped cesium iodide (CsI) scintillator and active matrix array.

Figure 2.14 shows a 3D rotational angiography system (3DRA). Images of the blood vessels can be

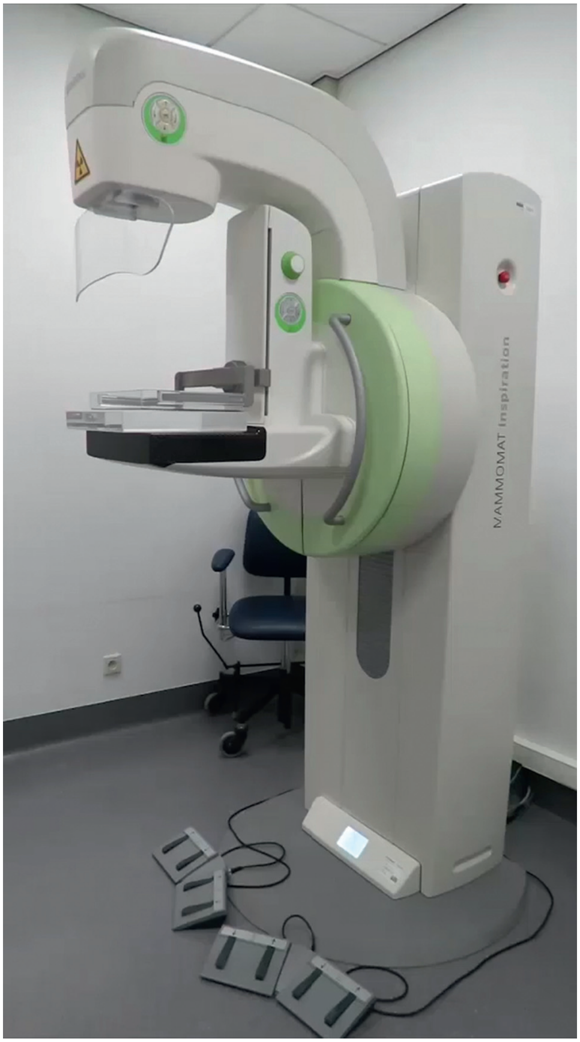

Figure 2.13 Digital mammography system employing direct X-ray conversion with amorphous selenium (Mammomat Inspiration, Siemens Healthcare). This system can also be used for digital tomosynthesis by rotating the X-ray tube from left to right (see Section 3.7.1).

made from any orientation by rotating the C-arm on which the X-ray tube and image detector are mounted at both ends. By continuously rotating the C-arm over a large angle (180° and more), sufficient projection images are obtained to reconstruct the blood vessels in three dimensions (3D) (Figure 2.15). The mathematical procedure used to calculate a 3D image from its projections is also used in CT and is explained in Chapter 3.

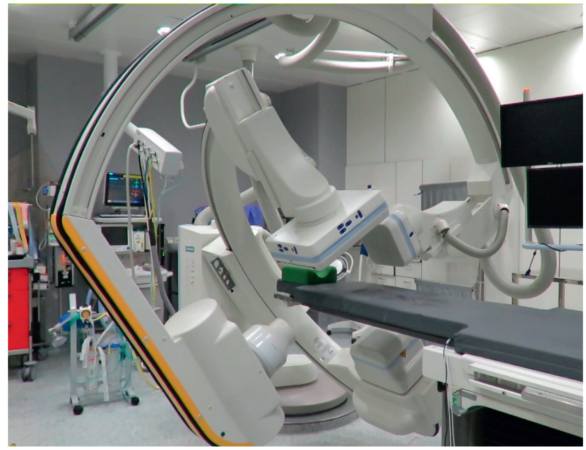

Figure 2.14 Biplane 3D rotational angiography (3DRA), consisting of a floor-mounted and a ceiling-mounted system both equipped with an X-ray tube and an active matrix flat panel detector (Artis zee biplane, Siemens Healthcare). The floor-mounted system acquires up to 7.5 fps (frames or images per second) at full spatial resolution (2480 x 1910 pixels). To reconstruct a 3D image of the blood vessels, a series of projection images is acquired at 60 fps while rotating the C-arm on a circular arc around the patient.

2.7 Clinical Use

Today, the majority of the radiographic examinations in a modern hospital are performed digitally. X-ray images can be static or dynamic. Static or still images can be made with any detector, whereas dynamic images are obtained with an image intensifier or an active matrix flat panel detector with fast readout. Dynamic image sequences are commonly known as fluoroscopic images as against radiographic images, which refer to static images.

In X-ray images, the attenuation differences of various nonbony matter are usually too small to distinguish them. A contrast agent or dye (i.e., a substance with a high attenuation coefficient) may overcome this problem. It is especially useful for intravascular (blood vessels, heart cavities) and intracavitary (gastrointestinal and urinary tract) purposes.

Following are a number of typical examples of frequently used examinations. They are subdivided into radiographic images and fluoroscopic images.

Radiographic images These are made of all parts of the human body. They are still responsible for the majority of radiological examinations. The most common investigations include the following:

– skeletal X-rays (see Figure 2.16).